

---

# Effect of Particle Shape on Unconfined Yield Strength

By: Dr. Kerry Johanson  
Material Flow Solutions, Inc.

---

NOTICE: This is the author's version of a work accepted for publication by Elsevier. Changes resulting from the publishing process, including peer review, editing, corrections, structural formatting and other quality control mechanisms, may not be reflected in this document. Changes may have been made to this work since it was submitted for publication. A definitive version was subsequently published in Powder Technology, Vol. 194, Issue 3, 15 September 2009, Pages 246-251, doi:10.1016/j.powtec.2009.05.004.

## Abstract

Unconfined yield strength is a property that influences many processes that handle bulk powder materials. Understanding which particle scale properties affect strength will help engineers design better products prior to production, reducing costly mistakes and increasing productivity. This paper examines the relationship between bulk unconfined yield strength and particle shape. It is an experimental work that suggests that the number of particle contacts per adjacent particle and the direction of these contacts are key parameters influencing the bulk strength. This paper suggests a way that shape effects can be incorporated in predictive models relating strength to particle scale parameters.

## Key Words

Unconfined yield strength, powder mechanics, adhesion, cohesion, shear, particle shape

## Introduction

Understanding bulk flow properties is critical to understanding process behavior. Typically, there are three phenomena that create troublesome behavior in industrial processes. First, cohesive materials cause stagnant regions or flow stoppages in process equipment. Second, material may segregate, creating a mixture with varying quality as material flows from process equipment. Finally, material may flow from process equipment at uncontrolled or erratic flow rates. There is one common flow property that affects all three of these process problems. This flow property is the unconfined yield strength, which is defined as the major principle stress that causes an unconfined bulk material to fail in shear. The tendency for a material to arch over outlets and form ratholes in process equipment is directly proportional to the unconfined yield strength [1]. Unconfined yield strength governs the stress holding material together on a free surface. It is the major principle stress that acts in a direction parallel to the free surface which supports the external forces tending to tear the surface apart [2]. In an arch, this free surface spans the outlet. In a rathole, this free surface is the surface of the pipe shaped channel that forms during discharge. If the strength is large enough to support the stress around the perimeter of the rathole, then the rathole remains stable, causing material to cling to the container surface and resulting in significant stagnant region formation around a central flow channel. In process equipment, piles form during filling discharge and in some cases during operation, such as in a rotary shell blender [3]. A pile is a free surface. The thickness of the avalanche layer is

dependent on the unconfined yield strength of the bulk material [4]. Thus, processes that form piles are, in part, controlled by the degree of cohesion in the bulk material. Segregation often occurs during pile formation [5]. Thus, anything that controls pile formation will also affect segregation tendencies. The ability of a given material to stick together often mitigates segregation tendencies [6]. Often erratic flow problems in process equipment occur due to excess air stored in the material [7], rathole collapse [8], or the sudden movement of stagnant material. In addition, the ability of gas counter-flow to fluidize material depends on how cohesive material is. Geldhart class C materials are cohesive and difficult to fluidize, forming channels rather than bubbles [9], [10], [11]. Unconfined yield strength can also be thought of as the resistance to shear of an assembly of particles. Several models have been proposed to relate the particle scale properties to the bulk unconfined yield strength. These are summarized in Table I below.

**Table 1 – Relationship Between Unconfined Yield Strength and Particle scale Properties**

Model	Mechanism	Source
$fc = \frac{K_1}{Dp^2}$	Van der Waals forces	Mollerus [12]
$fc = \frac{K_2 \cdot \sqrt{C}}{Dp}$	Capillary forces	Rabinovich [13]
$fc = \frac{K_3}{Dp^{1/2}}$	Elastic fracture	Rumpf [14]
$fc = \frac{K_4}{Dp^n}$	Plastic-elastic fracture	Specht [15]

It is important to point out that relationships in Table 1 are for perfectly spherical particles that have uniform particle size. None of these relationships contain the effect of particle shape or size distribution. This paper examines the effect particle shape has on the bulk unconfined yield strength.

### Experimental Methods

One of the difficulties of conducting a study of shape effects on yield strength is the ability to obtain a consistent sample of distinct shapes that poses strength as a bulk. This work uses plastic pellets of different shapes (round, heart, and stars) coated with soft Tacky Wax from Yaley Enterprises to make them cohesive (Figure 1). A prescribed amount of Tacky Wax was placed in premeasured samples of three different shaped pellets. These pellets and wax were heated to 50°C and mixed for about 30 minutes to create three distinct mixtures with 2.02% ± 0.06% by weight Tacky Wax. These mixtures were then cooled to 21°C before measuring the strength of the bulk. The uniformity of the coating on each pellet shape was determined by measuring the deviation in weight of 100 coated pellets for each of the three shapes and comparing this value to the deviation in weight of 100 non-coated pellets. This analysis suggested nearly uniform wax coatings occurred on the pellets. For example, consider the heart shaped pellets. On average these coated pellets varied in weight by 3.37% and the non-coated pellets varied in weight by 3.19%. This difference in pellet variation implies that the coating of Tacky Wax causes an

additional variation of about 0.18% in pellet to pellet weights for heart shaped pellets. This variation represents less than 10% of the total concentration of the 2.02% Tacky Wax on the sample. The other two pellet shapes showed similar results. This suggests that the coated materials have a reasonably uniform coating of Tacky Wax on each particle and the 30 minute mixing time is sufficient to create a representative sample.



**Figure 1. Typical Pellets Used in this Analysis**

There are a variety of test techniques that can measure bulk unconfined yield strength [16], [17], [18], [19]. The direct shear methods such as the Schulze method or Jenike method require the material to have small particle sizes to generate good data. The Johanson uniaxial tester can give an approximation to the unconfined yield strength with one sample and can give reasonable results with larger particles. Literature suggests that the standard 5-cm diameter test cell can work with 0.5-cm diameter particles. The Johanson uniaxial test method was used with a 10-cm test cell suggesting that reasonable results are possible with particles as large as 1-cm in diameter. The uniaxial method also allows very good control of the stress level applied to the material. Ten repeat measurements of unconfined yield strength at a series of consolidation pressure were taken, averaged, and plotted as a function of compaction pressure (Figure 2). Error bars for data in this plot was omitted for clarity but used in figures later in this paper.

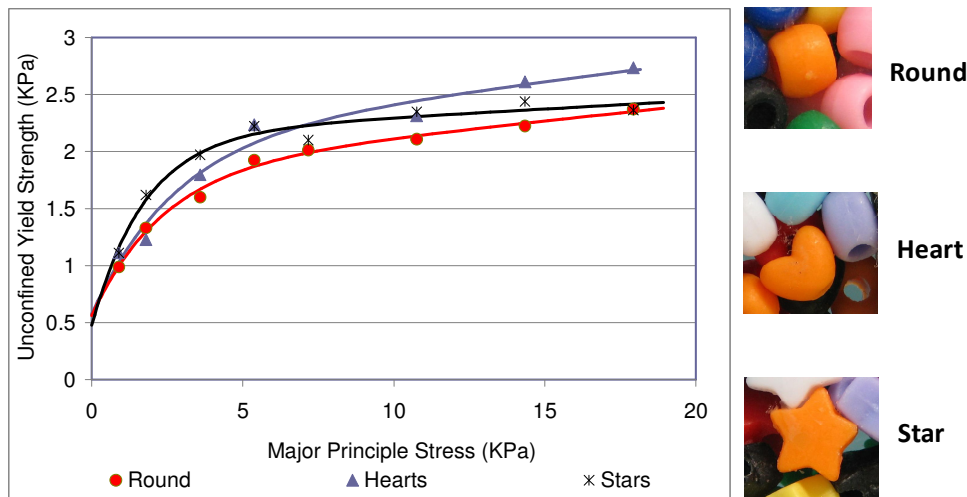


**Figure 2. Unconfined yield strength of various shaped particles as a function of consolidation pressure.**

The round particles appear to gain strength quickly as consolidation pressure is increased and level off at higher consolidation pressures. The hearts appear to have very similar strength values to the round particles at low consolidation pressures, but have larger strength values at higher consolidation pressures. The stars appear to have the same strength as the round particles at low consolidation pressures, but increase strength quicker than round particles as

consolidation pressure increases, and then level off to about the same value as the round particles at high consolidation pressures. The purpose of this paper is to examine the differences between these strength values and determine if some characteristic of the particle shape could explain this behavior. One of the obvious potential differences between these particles is the possibility that non-spherical particles could have multiple contacts between the same two particles. In the case of non-spherical particles two adjacent particles may have more than one contact point cementing the particles together as shown in Figure 3.



**Figure 3. Typical particle contacts between adjacent particles**

It is obvious from these particles that there is only one contact point between particles 1 and 2. However, there are two contact points between particles 2 and 3. One interpretation of unconfined yield strength is that strength is the initial resistance of a bulk material to shear caused by the integrated effect of all the individual forces acting between adjacent particles in the shear zone. The forces existing between particles are divided into two categories. Some of those forces are adhesive forces and some are frictional forces (Figure 4). The particle above these two adjacent particles is moving to the left during shear, which induces a friction force  $F_{frict}$  on the moving particle. There is also a normal force  $F_{norm}$  acting on the moving particle at this frictional contact point. There are external forces ( $F_x$  and  $F_y$ ) that act in the x and y direction on the particle, caused by other particles in the neighborhood. Finally there are adhesion forces  $F_{ad}$  which act to bind adjacent particles together and provide a pulling resistance as the top particle moves towards the left.

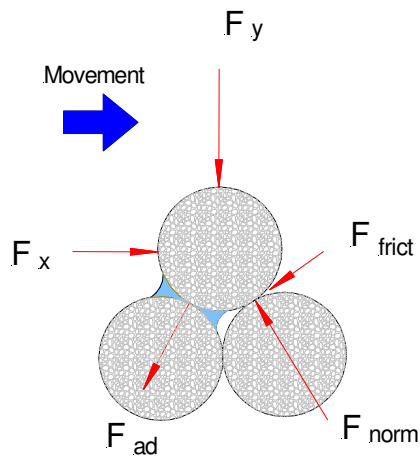


**Figure 4. Typical forces acting on a particle in shear**

Suppose strength is caused by the number and type of adhesion points between adjacent particles. If one could count the number of contacts between adjacent particles and estimate the relative magnitude of contact forces, then one could compare the strength of particles with single contacts between particles and the strength of particles that have multiple contacts between adjacent particles. The fact that the coating is the same in these three systems suggests that the contact forces on all particles are roughly the same (excluding any particle curvature issues). One would then expect the unconfined yield strength to scale with the number of contacts in a given unit volume. Thus, if one could estimate the number of total contacts in a given unit volume, then a correction factor accounting for the number of contacts could be used to relate the spherical particle unconfined yield strength to the non-spherical particle unconfined yield strength. The challenge is that material is subjected to shear (inter-particle motion) during measurement of strength. In fact, strain imposed during shear testing using the uniaxial strength tester was about 16%. This is further complicated by the fact that this strain occurs at a prescribed stress condition. Ideally we would like to measure the number of contacts as a function of both the stress and strain placed on the material. A special test cell was constructed that allowed material to be strained at a prescribed contact pressure. The cell consisted of a series of hinged plates placed in between two sheets of glass to form a rhombus shaped boxed (Figure 5). Material was placed in the box between these two glass sheets and a piston was placed on top of this material. A load was applied to the box while the bottom of the box oscillated back and forth to induce strain. The piston provides the pivot point allowing the box to change from a square to a rhombus and back again.

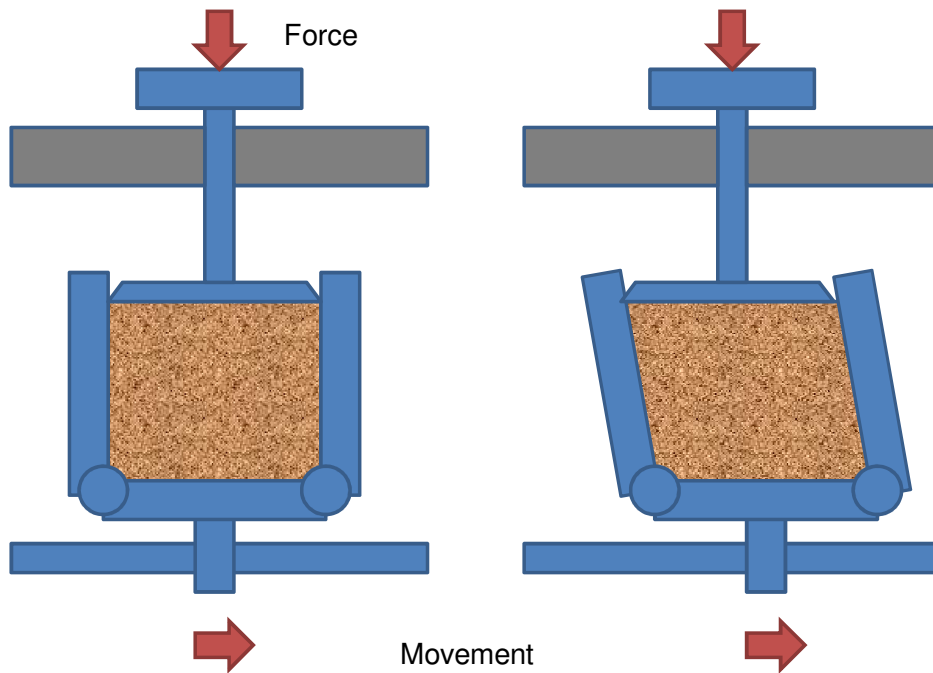


**Figure 5. Pure Shear Box (front view)**

The total shear ( $\gamma$ ) in the box is computed from the maximum extension angle ( $\theta_w$ ) of the side walls and the number of cycles ( $N_{cyc}$ ) (see equation 1).

$$\gamma = 4 \cdot N_{cyc} \cdot \tan(\theta_w) \quad (1)$$

The pellets were placed in this test cell and strain induced while a constant load was placed on the piston. The front of the test cell was clear and allowed visualization of the pellets in the tester. After the material was subjected to a given strain at a prescribed consolidation load, pictures were taken of the particle assembly in the tester and the number of contacts between adjacent particles was recorded through manual visual inspection of these pictures. Contact information was measured for about a hundred particles of each particle shape. Strength is dependent on the forces causing adhesion between particles. These are vector forces and when two or more contacts exist between two adjacent non-spherical particles the forces cannot act along the axis that joins the two particle centers. These two contact forces could be replaced with a single force acting through the center of the particle and, potentially, an external moment or screw term. This extra moment term is caused by the fact that the forces do not need to pass through the center of the particle and can result in a net moment acting about some axis in space. We will neglect this moment or screw term, but we can easily adjust the contact data to account for the fact that only the component of the normal adhesion forces acts in a direction parallel to a line, connecting two adjacent particles together. This has the net effect of reducing the pull-off force between two adhering particles (Figure 6). The images collected of the particle assembly were also optically analyzed using software called ImageJ to determine the angle of these contacts relative to the particle-to-particle centroids.

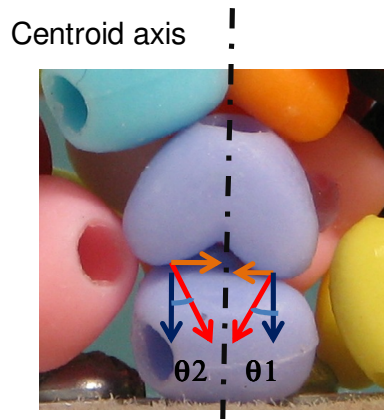


**Figure 6. Effective contact force correction for multiple contacts**

If it is assumed that each normal contact results in identical forces, then the average correction factor for force in the direction of particle-to-particle contact (along the centroid axis) is defined by equation 2. The number of contacts would be multiplied by this correction factor to obtain the effective number of contacts for computing strength correction terms.

$$Cf = \frac{\cos(\theta_1) + \cos(\theta_2)}{2} \quad (2)$$

The average number of contacts per adjacent particle was measured as a function of stress at a strain value of about 16% (about 0.23 cycles at an extension angle of 10 degrees). The angles ( $\theta_1, \theta_2$ ) of each contact relative to the centroid axis was also measured and the correction factor ( $Cf$ ) was computed. These values for all contacts were averaged over all the particles imaged.

The net result is a relationship between the stress level and the effective number of contacts between particles (Figures 6 and 7). This number must be greater than 1.0 suggesting that, on average, more than one particle contact per adjacent particle may exist. It is important to note that the number of contacts per adjacent particle for round shaped particles is always 1.0. However, different shapes can have contact numbers greater than 1.0. For example, it is clear from Figure 6 that the stress level does not change the number of contacts per adjacent particle with heart shaped particles, giving 15%-20% more contacts than would be expected in a spherical system. If just the number of contacts is considered, then the average number of contacts per adjacent particle ranges between 1.2 and 1.15 depending on the stress level applied for heart shaped particles. If the direction of these contacts is included in the analysis, then the number of effective contacts per adjacent particle decreases to between 1.15 and 1.11 depending on the stress level.

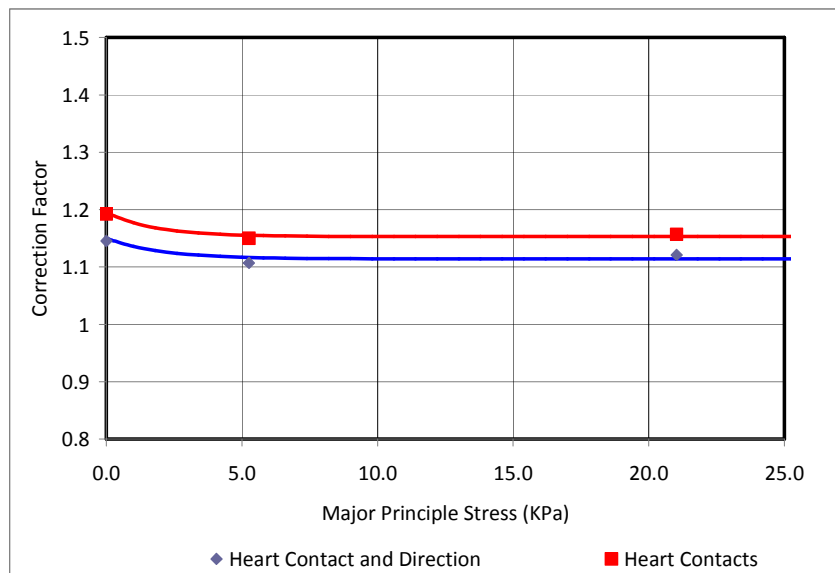


**Figure 7. Number of contacts as a function of stress at 16% strain for heart shaped particles**

The same analysis was carried out for star shaped particles. If just the numbers of star particle contacts are considered, then the average number of contacts per adjacent particle ranges between 1.42 and 1.14, depending on the stress level applied to the star shaped particles. If the direction of these contacts is included in the analysis, then the number of effective contacts per adjacent particle varies between 1.30 and 1.10, depending on the stress level. This material shows a large stress effect on the number of contact point per adjacent particles. The reason for this effect is that, in the star particle system, two preferred structures occur. One structure causes the stars to line up with the flat star surfaces parallel to each other, resulting in a single contact point per adjacent particle. The other stable configuration is where the tips of stars interlock, forming multiple contacts. The imposed shear causes the particle to rotate and forces a predominance of flat-to-flat contacts as shear and stress level are increased. Once the flat star surfaces are in contact, further rotation is difficult. Thus, the effective number of contacts decreases at high stress levels (Figure 8).

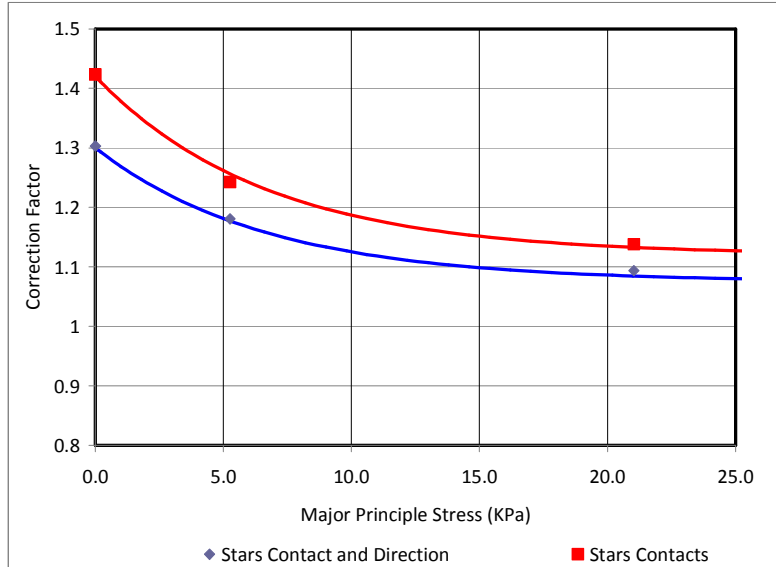


**Figure 8.** *Number of contacts as a function of stress at 16% strain for star shaped particles*

These correction factors can be used as direct multiplicative factors to estimate the strength of a non-spherical particle system given data from round particles. Multiplying the strength measured for the round particles by the effective number of contacts in the heart shaped particle system leads to an approximation of the data measured from the uniaxial shear cell (Figure 9). The computed heart strength curve fits the data well at high consolidation pressures, but shows some deviation at lower consolidation pressures. When the direction of heart particle contacts is included in the calculation, then the data over the entire range of stress levels compares well with experimental measurements (Figure 10). This suggests that unconfined yield strength is a function of both the number of particle contacts per adjacent particle, and the direction of those particle contacts.

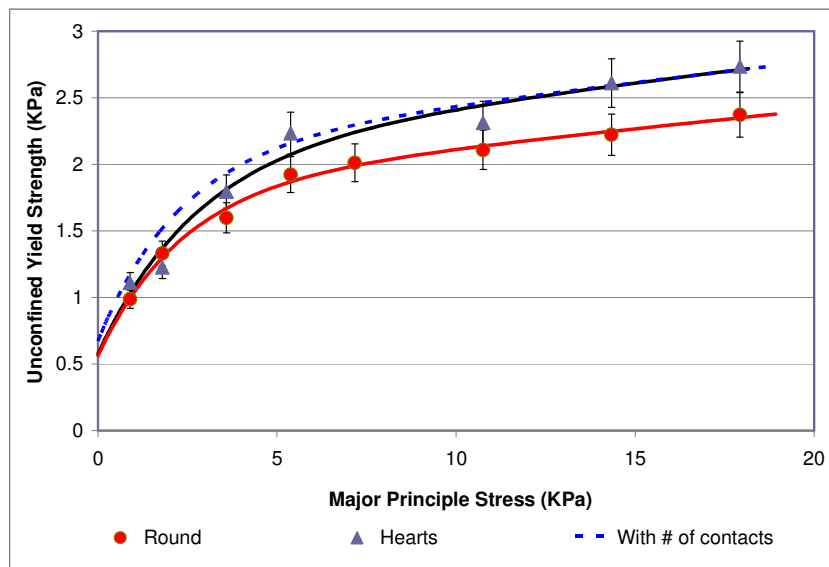


**Figure 9.** *Correction factor applied to round particle strength to correct for the number of contacts per adjacent particle for heart shaped particles*

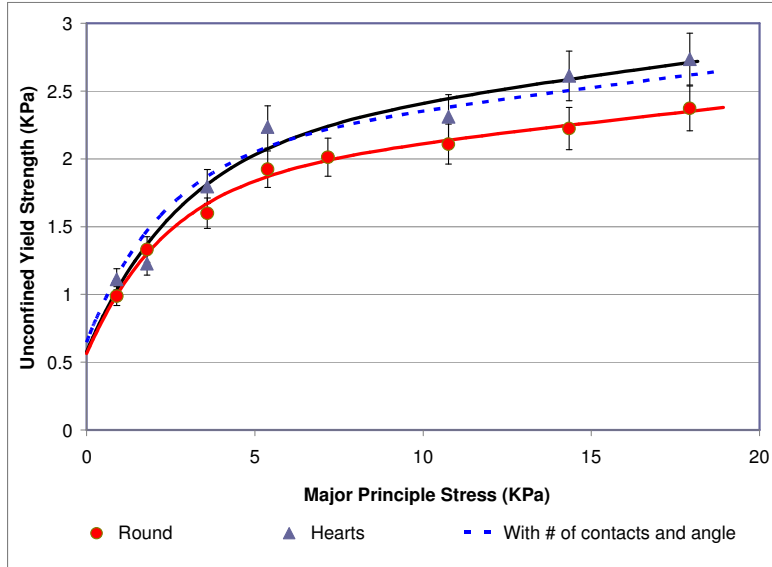


**Figure 10.** *Correction factor applied to round particle strength to correct for the number of contacts and the direction of the contact per adjacent particle for heart shaped particles*

This same analysis was done with star shaped particles. Multiplying the strength measured for the round particles by the effective number of contacts in the star shaped particle system leads to an approximation of the data measured from the uniaxial shear cell (Figure 11). However, the computed star strength curve does not fit the data well and predicts high values. Including the direction of star shaped particle contacts lowers the prediction and results in a prediction fitting the experimental results for most of the lower solid stress level region. There appears to be some deviation at the larger stress levels, suggesting this simple analysis requires some additional modification to explain the observed data (Figure 12). However, the fit is good enough to defend the suggestions that two key parameters influencing strength of a bulk powder system are the number of contact per adjacent particles and the direction of these contacts relative to the centroid axis between adjacent particles. Further work needs to be done to generalize this to any system with variable particle shapes. This will be the subject of another paper.

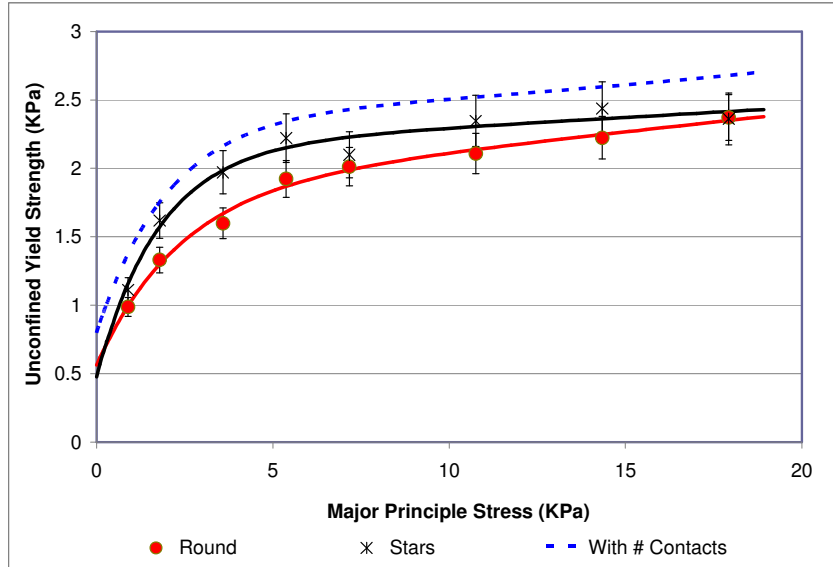


**Figure 11.** Correction factor applied to round particle strength to correct for the number of contacts per adjacent particle for star shaped particles

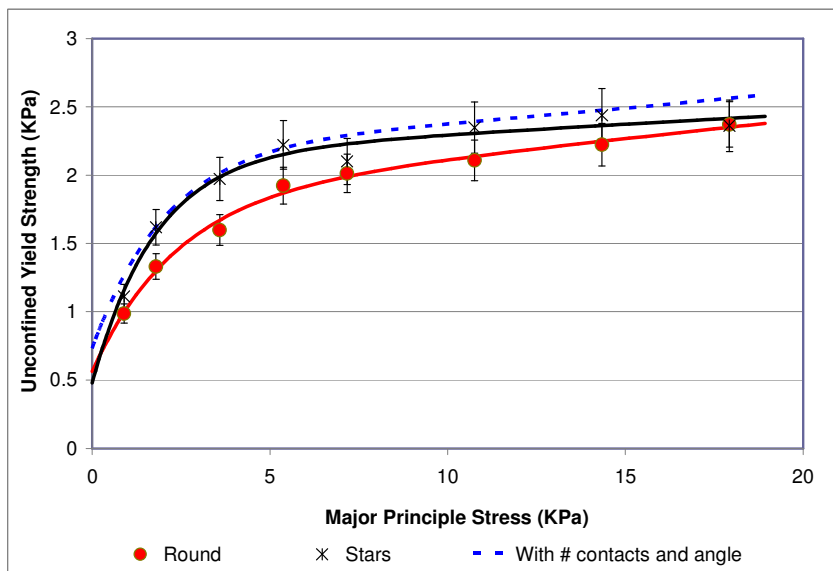


**Figure 12.** Correction factor applied to round particle strength to correct for the number of contacts and the direction of the contact per adjacent particle for star shaped particles

### Summary

The important results from this work are that the number of contacts per adjacent particle and the direction of these contacts are key factors which influence the bulk strength of material. This work also suggests that simple models including these effects may be useful in predicting bulk unconfined yield strength for particle scale properties. Future models describing yield strength of bulk materials should consider incorporating these two effects. The limitation of this

approach is that it requires measured strength data for an ideal system. However, once the ideal system is characterized, then the technique outlined above can be implemented to predict non-ideal systems. The strength of this approach is that, if one could develop models predicting strength in ideal systems from just particle scale properties, then the approach used in this paper would help extend the ideal system to non-ideal conditions, thereby bridging the gap between real world materials and idealized systems. The next step should be to extend this analysis to smaller particle systems and general shape systems.

## Nomenclature

$f_c$	is the unconfined yield strength of the bulk material
$D_p$	is the particle size
$C$	is the moisture content
$C_f$	is the correction factor to account for the number of contacts broken during a shearing event
$F_x$	is the external particle force acting in the x-direction
$F_y$	is the external particle force acting in the y-direction
$F_{ad}$	is the adhesion force acting between particles
$F_{frict}$	is the friction force acting between particles
$F_{norm}$	is the normal contact force at friction contacts
$K_1$	is a Van der Waals proportionality function
$K_2$	is a capillary bond proportionality function
$K_3$	is an elastic fracture proportionality function
$K_4$	is an elastic/plastic proportionality function
$N_{cyc}$	is the number of shear cycles
$\theta_w$	is the extension angle in the shear box
$\theta_1$	is the 1 <sup>st</sup> contact angle relative to the centroid axis
$\theta_2$	is the 2 <sup>nd</sup> contact angle relative to the centroid axis
$\gamma$	is the strain in the shear box

## Acknowledgements

The author acknowledges the financial support of the Particle Engineering Research Center (PERC) at the University of Florida, The National Science Foundation (NSF Grant EEC-94-02989), Material Flow Solutions Inc. and the Industrial Partners of the PERC for support of this research.

## References

1. Jenike, A.W., Storage and flow of solids, Bulletin No. 123, University of Utah Engineering Experiment Station, November 1964.
2. Jenike, A.W., Gravity flow of bulk solids, Bulletin No. 108, University of Utah Engineering Experiment Station, 1961.
3. Moakher, M., T. Shinbrot and F.J. Muzzio, Experimentally validated computations of flow, mixing and segregation of non-cohesive grains in 3D tumbling blenders, *Powder Technology*, 109 (1-3), p. 58-71, 2000.

4. Chaudhuri, Bodhisattwa, Amit Mehrotra, Fernando J. Muzzio, M. Silvina Tomassone, Cohesive effects in powder mixing in a tumbling blender, *Powder Technology*, 165, p.105–114, 2005.
5. Johanson, Kerry, Chris Eckert, Dev Ghose, Millorad Djomlija, Mario Hubert, Quantitative measurement of particle segregation mechanisms, *Powder Technology*, 159 1 – 12, 2005.
6. Johanson, Jerry R., Ph.D., Solids segregation: causes and solutions, *Powder and Bulk Engineering*, August, 1988.
7. Rathbone, T. and R. M. Nedderman, The deaeration of fine powders, *Powder Technology*, 51, 115, 1987.
8. Bell, Timothy A., Challenges in the scale-up of particulate processes – an industrial perspective, *Powder Technology*, Volume 150, Issue 2, p 60-71, February 2005.
9. Wes, G. W. J., S. Stermerding and D. J. van Zuilichem, Control of flow of cohesive powders by means of simultaneous aeration, and vibration, *Powder Technology* Volume 61, Issue 1, p. 39-49, April 1990.
10. Brunia, Giovanna, Paola Lettieria, David Newtonb, and Diego Barletta, An investigation of the effect of the inter-particle forces on the fluidization behaviour of fine powders linked with rheological studies, *Chemical Engineering Science*, Volume 62, Issues 1-2, p. 387-396, January 2007.
11. Wang, Zhaolin, Mooson Kwauk, and Hongzhong Li, Fluidization of fine particles, *Chemical Engineering Science*, Volume 53, Issue 3, p. 377-395, February 1998.
12. O. Molerus, The role of science in particle technology, *Powder Technology*, Volume 122, Issues 2-3, 22, p. 156-167, January 2002.
13. Rabinovich, Y., M. S. Esayanur, K. Johanson, B. Moudgil, Oil mediated particulate adhesion and mechanical properties of powder, *Proceedings World Congress on Particle Technology*: paper 370, 2002.
14. Rumpf, H., *Particle Technology*. New York: Chapman and Hall, 1990.
15. Specht, D., Caking of granular materials: an experimental and theoretical study, Thesis, University of Florida, 2006
16. de Silva, S.R., Characterization of particulate materials – a challenge for the bulk solid fraternity, *Powder Handling & Processing*, December 2000.
17. Van der Kraan, M., Techniques for the measurement of flow properties of cohesive powders, Thesis, University of Delft, 2000.
18. Johanson, J.R., The Johanson indicizer system vs. the Jenike shear tester, *Bulk Solids Handling*, 12(2), p. 237-240, 1992.
19. Peschl, I.A.S.Z., Quality control of powders for industrial application, *Proceedings of 14<sup>th</sup> annual Powder & Bulk Solids Conference*, Chicago, p. 517-536, 1989.